

Scattering coefficient determination in turbid media with backscattered polarized light

Franck Jaillon

Hervé Saint-Jalmes

Université Claude Bernard Lyon

1 CNRS UMR 5012-CPE

Laboratoire de Résonance Magnétique Nucléaire

La Doua 3, rue Victor Grignard

69616 Villeurbanne, France

Abstract. A simple empirical method is presented to determine the scattering coefficient μ_s from backscattered polarized images of turbid media. It uses the ratio, pixel by pixel, of two images that are the second and the first backscattered Stokes parameter images Q and I , respectively. Taking this image ratio, then integrating it over the azimuth angle, we get a function depending on the distance from the light entrance point. This function has a maximum. Using Monte Carlo simulations, for a fixed reduced scattering coefficient μ_s' and for an anisotropy factor g varying between 0 and 0.8, it is found a linear relationship between the scattering coefficient μ_s and the inverse of the maximum position of this function. © 2005 Society of Photo-Optical Instrumentation Engineers. [DOI: 10.1117/1.1924715]

Keywords: polarization; backscattering; Mie theory; multiple scattering; photon migration; turbid media.

Paper 04013 received Feb. 4, 2004; revised manuscript received Sep. 30, 2004; accepted for publication Dec. 20, 2004; published online Jun. 7, 2005.

1 Introduction

During the 1990s the use of nonpolarized backscattered light has made it possible to optically characterize turbid media with noninvasive measurements. By characterization, we mainly refer to the determination of the mean transport scattering coefficient μ_s' and the absorption coefficient μ_a with spatially resolved techniques.¹ Models² were generally developed from the radiative transfer equation. Then, thanks to polarized light, several studies³⁻⁵ showed that backscattered polarized light contains information that was more localized and dependent on the scattering coefficient μ_s . It was also demonstrated⁶ that linearly polarized light propagates through a smaller region than the circular one. We concentrate here on the second parameter of the backscattered Stokes vector, that is Q , in the case of linearly polarized incident light. This parameter represents the intensity difference between the parallel and perpendicular polarization direction. Parallel (respectively perpendicular) direction means that the analyzer direction is parallel (respectively perpendicular) to the polarizer one. The purpose of this paper is to utilize polarization backscattered patterns from turbid media to determine the scattering coefficient μ_s . The first part presents an experimental test of the method on polystyrene microspheres. Then, in order to determine the limits of the proposed method with respect to the reduced scattering and absorption coefficients, μ_s' and μ_a , respectively, Monte Carlo simulations are realized.

2 Experimental Method

The experimental setup (see Fig. 1) is composed of a laser diode that has a 670 nm wavelength and a 5 mW power. The

beam passes through a polarizer and is directed to the sample. The incidence angle is $\theta=15^\circ$. The sample which is composed of calibrated polystyrene microspheres (Merck) then scatters light to an analyzer positioned in front of a 16 bit CCD camera. The backscattered image is recorded by a CCD matrix (ICX084L HyperHAD, Sony) made of 659×494 pixels, each pixel measuring $7.4 \mu\text{m}$.

Here we only focused on the first and second Stokes parameters I and Q , respectively, using linear polarizers. The Stokes vector is defined as follows:

$$\mathbf{S} = \begin{pmatrix} I \\ Q \\ U \\ V \end{pmatrix} = \begin{pmatrix} E_{\parallel}E_{\parallel}^* + E_{\perp}E_{\perp}^* \\ E_{\parallel}E_{\parallel}^* - E_{\perp}E_{\perp}^* \\ E_{\parallel}E_{\perp}^* + E_{\perp}E_{\parallel}^* \\ i(E_{\parallel}E_{\perp}^* - E_{\perp}E_{\parallel}^*) \end{pmatrix}, \quad (1)$$

thus, in order to get the second parameter, that is Q , we need to record two images. The first one is obtained with the analyzer parallel to the polarizer, that gives us $E_{\parallel}E_{\parallel}^*$ and the second one with the analyzer perpendicular to the polarizer, that provides $E_{\perp}E_{\perp}^*$. Finally the difference (respectively the sum) of these two images is the Q (respectively the I) Stokes vector element. Note that experimentally we also need to subtract the dark image to get rid of any possible camera intensity offset. The Q parameter is shown in Fig. 2 for a monodisperse sphere suspension that has a (360 ± 5) nm diameter and whose refraction index is 1.58. With the source wavelength and the refraction index of the medium ($n_{\text{water}}=1.33$), we compute⁷ an anisotropy factor g of 0.71. Further, because the concentration is 0.5%, we deduce the value of the scattering coefficient μ_s is equal to 59 cm^{-1} and the absorption coefficient μ_a is assumed to be null. The incident linear polarization is along the horizontal axis of the image.

Address all correspondence to Hervé Saint-Jalmes. Tel: 334 7243 1988; E-mail: saint-jalmes@univ-lyon1.fr

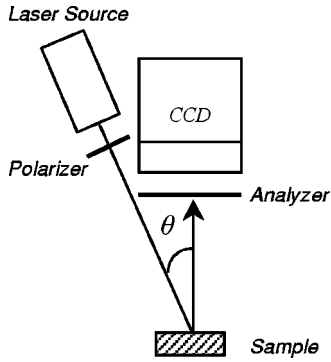


Fig. 1 Schematic diagram of the experimental setup.

We are interested here in the spatial extent of the vector element Q with respect to I . In other words, we want to know the typical size of the backscattered pattern. We thus integrate the image Q/I over the azimuth angle φ [see Fig. 3(a)] to only have a dependence in r , which is the distance from the entrance point of light. We call this integral $q(r)$:

$$q(r) = \int_0^{2\pi} \frac{Q(r, \varphi)}{I(r, \varphi)} d\varphi. \quad (2)$$

This function $q(r)$ is drawn in Fig. 3(b) for two sphere suspensions, that have different scattering coefficients μ_s of 28 and 39 cm^{-1} . The first feature of $q(r)$ shows that the spatial expansion is small with respect to the one of the intensity I that is generally of the order of several λ'_s , the transport mean free path. More interestingly this curve has a maximum, let us call l_m the distance corresponding to that maximum. For our two examples, namely $\mu_s = 28$ and 39 cm^{-1} , we have l_m that is equal to (0.033 ± 0.002) and (0.025 ± 0.002) cm, respectively. Thus, taking the inverse of these distances, we get (30 ± 3) and (40 ± 3) cm^{-1} , respectively, that corresponds to the scattering coefficient μ_s . In order to confirm that trend, let us look at the Monte Carlo simulations in order to see the influence on that method of the reduced scattering coefficient μ'_s and the absorption coefficient μ_a .

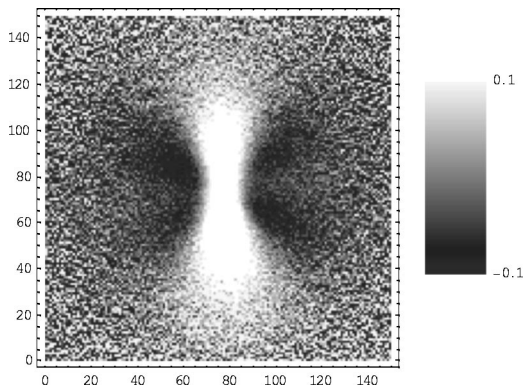


Fig. 2 Experimental Q/I image for a suspension of polystyrene spheres. Parameters: $g=0.71$, $\mu_s=59 \text{ cm}^{-1}$, $\mu_a=0 \text{ cm}^{-1}$. Image size $=0.57 \text{ cm} \times 0.57 \text{ cm}$.

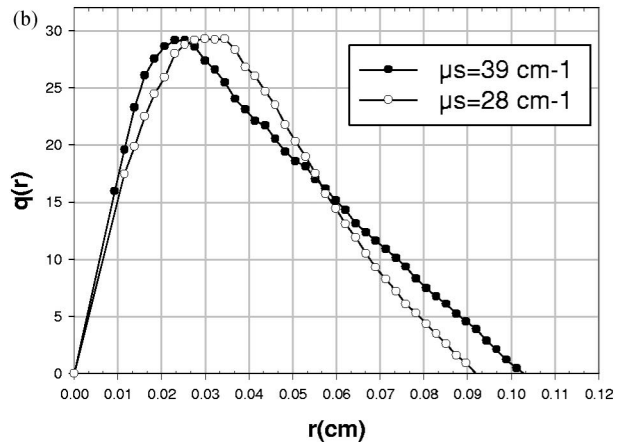
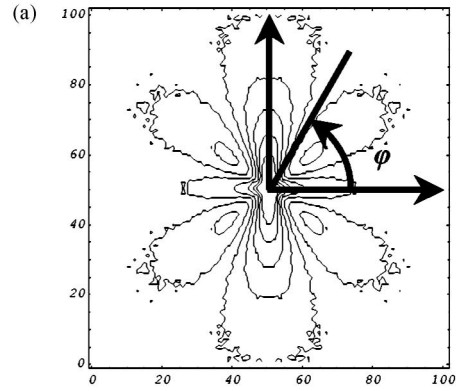


Fig. 3 (a) Azimuth angle φ for a Q/I image and (b) experimental $q(r)$ for two scattering coefficients $\mu_s = 28$ and 39 cm^{-1} .

3 Monte Carlo Simulations

The Monte Carlo code⁸ simulates the propagation of polarized light through a scattering medium having a slab shape, that is composed of homogeneously distributed spheres. This code considers a polarized light source illuminating one point of the turbid medium surface. This Monte Carlo simulation is based on a previous one⁹ that described propagation of unpolarized light thanks to the radiative theory using the absorption and scattering coefficients, μ_a and μ_s , respectively. In addition to the position of the photon and its propagation direction, the photon packet is characterized here by its Stokes vector which is defined in the photon local frame when this photon packet is inside the medium. Thanks to the Mie theory,¹⁰ we know the anisotropy factor g of the spheres and the Mueller matrix for a single scattering. This makes it possible to statistically generate the photon direction for each scattering. Thus, we follow the modification of the Stokes vector and as the photon escapes the medium, either in the backscattering case or the transmission one, this vector is expressed in the detector frame and recorded. Notice that the detector is assumed lying on the medium surface. We end up with a backscattering (and transmission) images for each element of the Stokes vector. An example of backscattering images is given in the Fig. 4 for the I and Q Stokes vector elements. The medium parameters are the following: $\mu_a = 0 \text{ cm}^{-1}$, $\mu_s = 57 \text{ cm}^{-1}$, $g = 0.65$, the thickness of the slab is $d = 0.5 \text{ cm}$, the sphere refractive index is $n_s = 1.58$, these

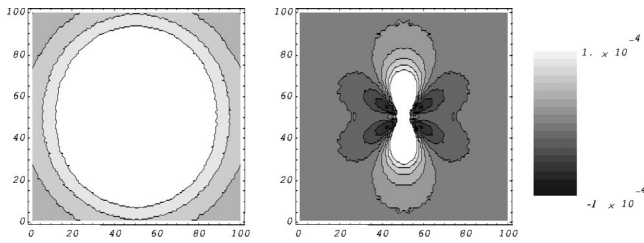


Fig. 4 Simulated backscattered I and Q images for a scattering medium with the following coefficients: $\mu_a=0 \text{ cm}^{-1}$, $\mu_s=57 \text{ cm}^{-1}$, $g=0.65$, thickness=0.5 cm, wavelength=670 nm. Image size 0.35 cm \times 0.35 cm.

spheres are immersed in a medium with a refraction index of $n_m=1.33$, and the source wavelength is equal to 670 nm. These images are normalized by the number of the photons used for that simulation, namely 100 millions. In our simulations, we set the value of the reduced scattering coefficient μ'_s equal to 20 cm^{-1} and we vary the value of the anisotropy factor g from 0.04 (equivalent to $\mu_s=21 \text{ cm}^{-1}$) to 0.8 (equivalent to $\mu_s=84 \text{ cm}^{-1}$). The absorption is still null. We follow the evolution of the inverse of the length l_m with respect to the scattering coefficient μ_s . The slab parameters are the following: medium refraction index $n_m=1.33$, sphere refraction index $n_s=1.58$, slab thickness $d=0.5 \text{ cm}$ and the source wavelength is 670 nm. The backscattered Q image is divided by the I image, pixel by pixel, and then integrated to obtain $q(r)$ (see Fig. 5). If we draw the maximum position l_m as a function of μ_s in the case where the anisotropy factor g varies between 0.04 and 0.8, we get the curve of the Fig. 6 where it can be seen a linearity between l_m and μ_s . The corresponding linear regression coefficient r^2 is equal to 0.985. The evolution of the relationship between l_m and μ_s is shown on Fig. 7 where the reduced scattering coefficient μ'_s has been changed to 10 and 40 cm^{-1} , respectively. We have a linear regression coefficient r^2 that is equal to 0.995 for $\mu'_s=10 \text{ cm}^{-1}$ and to 0.977 for $\mu'_s=40 \text{ cm}^{-1}$. Considering the coefficient r^2 , it is difficult to conclude on the influence of the transport scattering coefficient μ'_s on the linear relationship between $1/l_m$ and μ_s . But its dependence remains weak compared to the one with the anisotropy factor g .

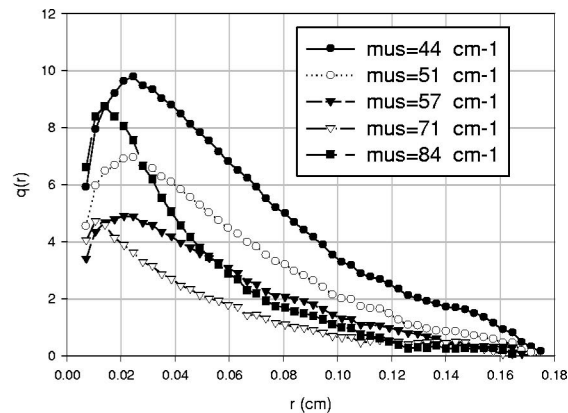
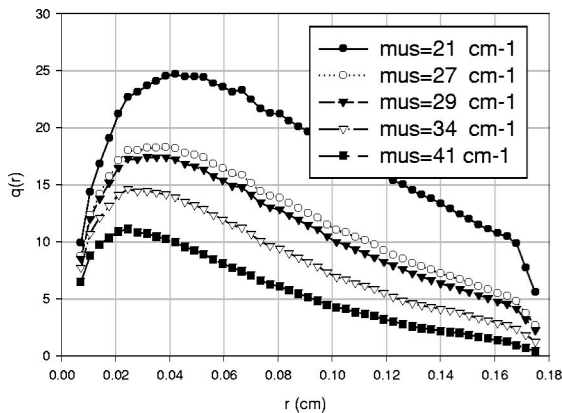


Fig. 5 Simulated $q(r)$ for different μ_s and with a constant $\mu'_s=20 \text{ cm}^{-1}$.

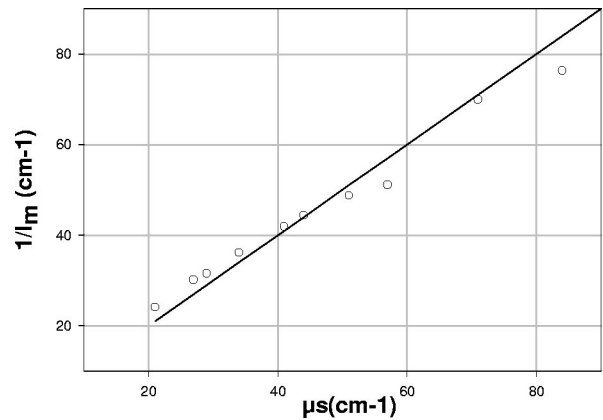


Fig. 6 $1/l_m$ with respect to μ_s (corresponding anisotropy factor g varies between 0.04 and 0.8). $\mu'_s=20 \text{ cm}^{-1}$. Linear regression coefficient $r^2=0.985$.

The influence of the absorption coefficient μ_a on the relationship between the maximum position l_m of $q(r)$ is shown on Fig. 8 when $\mu'_s=20 \text{ cm}^{-1}$, for two examples of absorption: $\mu_a=1$ and 5 cm^{-1} . The linear regression coefficient r^2 for the first example is 0.966 and 0.659 for the second case. Therefore considering the diminishing linear regression coefficient r^2 , the linearity between $1/l_m$ and μ_s disappears as the ratio μ_a/μ'_s increases. We notice that as the absorption increases there is a region (corresponding to $g < 0.7$) where the length l_m is smaller than expected.

4 Discussion

The advantage of this method is its weak dependence with the transport mean free path λ'_s in the case of a negligible absorption coefficient μ_a compared to μ'_s . These coefficients can be known, for example, with a reflectance technique using unpolarized light.¹¹ As the anisotropy factor g tends to 1, we see [Fig. 9(left)] that the distance l_m does not vary anymore. Its inverse tends approximately to the value of 80 cm^{-1} [Fig. 9(right)]. This cannot be explained by the thickness of the slab since the latter has been modified and increased to 10 cm in order to see if it influences the backscattered intensity as the anisotropy factor g increases to 1. The results of the simula-

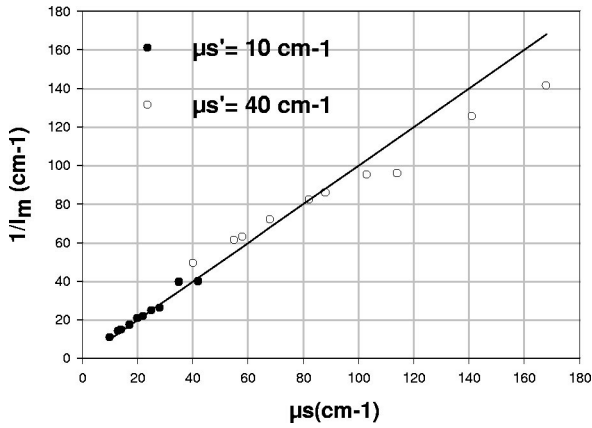


Fig. 7 $1/l_m$ with respect to μ_s . For $\mu'_s = 10 \text{ cm}^{-1}$, $r^2 = 0.995$. For $\mu'_s = 40 \text{ cm}^{-1}$, $r^2 = 0.977$. The corresponding anisotropy factor g varies between 0.04 and 0.8 for each transport scattering coefficient.

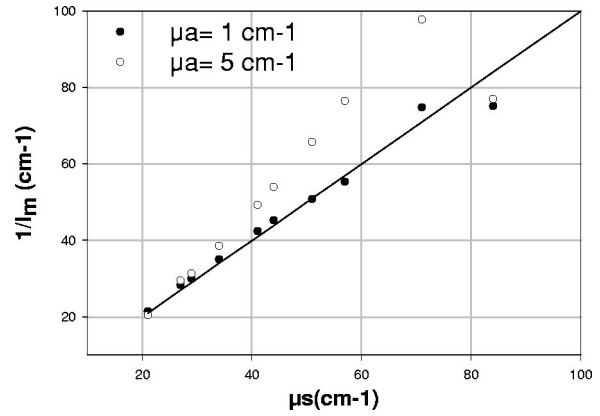


Fig. 8 $1/l_m$ with respect to μ_s for $\mu'_s = 20 \text{ cm}^{-1}$. For $\mu_a = 1 \text{ cm}^{-1}$, $r^2 = 0.966$. For $\mu_a = 5 \text{ cm}^{-1}$, $r^2 = 0.659$. The corresponding anisotropy factor g varies between 0.04 ($\mu_s = 21 \text{ cm}^{-1}$) and 0.8 ($\mu_s = 84 \text{ cm}^{-1}$) for each absorption coefficient.

tion, in the case where $g = 0.92$, give no difference concerning the behavior of the curve $q(r)$, that is the position of the maximum is not altered. Consequently, the distance l_m remains unchanged even if the thickness represents a large number of times (≈ 2500) the mean free transport λ'_s . An explanation can be given by the Mie distribution, that generates the propagation direction of the photons. Indeed if we assume a single scattering, we have the following Mueller matrix:

$$\begin{pmatrix} m_{11}(\theta) & m_{12}(\theta) & 0 & 0 \\ m_{12}(\theta) & m_{11}(\theta) & 0 & 0 \\ 0 & 0 & m_{33}(\theta) & m_{34}(\theta) \\ 0 & 0 & -m_{34}(\theta) & m_{33}(\theta) \end{pmatrix}, \quad (3)$$

where the elements depending of the polar angle θ of this matrix are defined by the Mie theory.¹⁰ If the initial polarization is linear, the incident Stokes vector can be chosen as $(1,1,0,0)$, and if we put the azimuth angle $\varphi = 0$, the scattered intensity I' is

$$I' = m_{11}(\theta) + m_{12}(\theta). \quad (4)$$

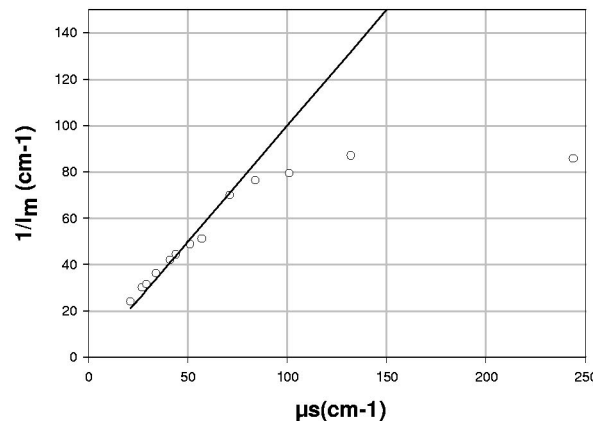
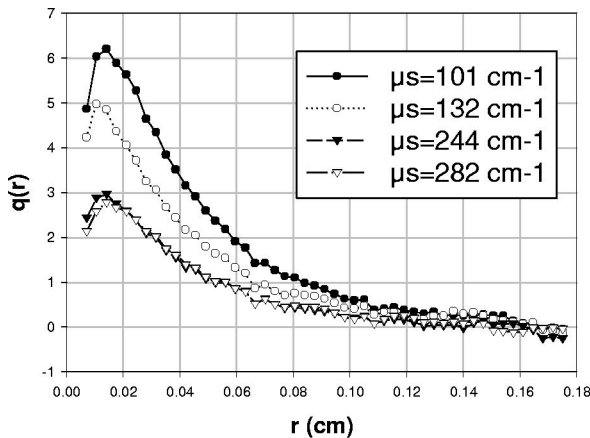


Fig. 9 (Left) $q(r)$ for different μ_s and with a constant $\mu'_s = 20 \text{ cm}^{-1}$, $\mu_a = 0 \text{ cm}^{-1}$ and (right) $1/l_m$ with respect to μ_s . $\mu'_s = 20 \text{ cm}^{-1}$ and $\mu_a = 0 \text{ cm}^{-1}$. Corresponding anisotropy factor g varies between 0.04 ($\mu_s = 21 \text{ cm}^{-1}$) and 0.93 ($\mu_s = 282 \text{ cm}^{-1}$).

Then we look, with respect to g , at the Mie distribution for a single scattering which means that $\theta = 180^\circ$ (see Fig. 10). To change g , we vary the radius of spheres, keeping constant the other sphere characteristics. We observe that this function is bijective with g if only the latter is under 0.65. Then the evolution of the Mie function tends to zero and the bijectivity disappears. That could explain the $q(r)$ behavior for high anisotropy factors.

We notice that if the integration over the azimuth angle is done on the backscattered image Q normalized by the total backscattered intensity I , the dependence of $1/l_m$ with respect to μ_s is not seen. We therefore need to combine the spatial evolutions of both Stokes vector element images I and Q by dividing them pixel by pixel. Moreover, since we consider lengths that are of the order of λ_s , an experimental problem that can occur is the entrance diameter of the light beam which will modify the backscattered image near the entry point. Thus the profile of the light source has to be known in order to correctly deconvolute the image and to get rid of the beam finite size influence.

Model describing qualitatively low scattering backscat-

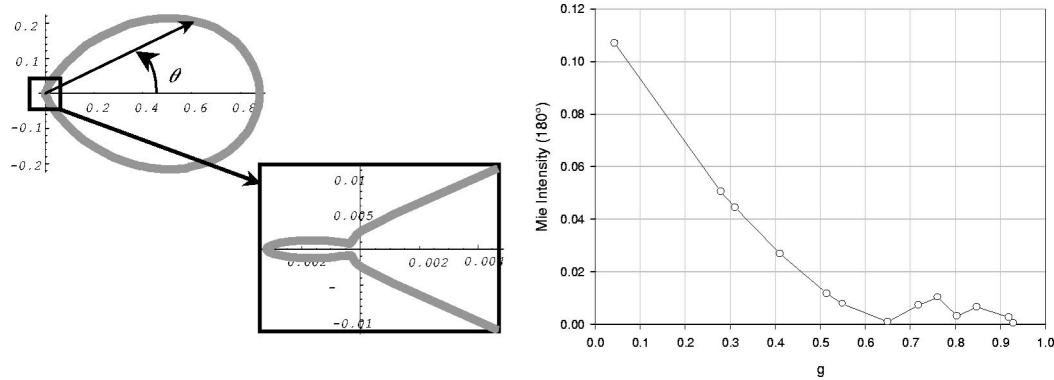


Fig. 10 (Left) Example of Mie intensity drawn in a polar plot and (right) variations of the Mie intensity for $\theta=180^\circ$ with respect to g .

tered polarized light already exists.¹² In order to extend this method for higher anisotropy factors, it is necessary to have a quantitative model that precisely describes the polarized backscattered light.

5 Conclusion

Thanks to experiments and Monte Carlo simulations, we have seen that the spatial information contained in the backscattered image ratio Q/I allowed to see the influence of the scattering coefficient μ_s and to determine the latter when the anisotropy factor g ranges between 0 and 0.8. A quantitative theoretical model is necessary to understand the multiple scattering regime and to be able the treatment of higher anisotropy factors, in order to be closer to biological tissue conditions.

References

1. A. Kienle and M. S. Patterson, "Improved solutions of the steady-state and the time-resolved diffusion equation for the reflectance from a semi-infinite turbid medium," *J. Opt. Soc. Am. A* **14**, 246–254 (1997).
2. T. J. Farrell, M. S. Patterson, and B. Wilson, "A diffusion theory model of spatially resolved, steady-state diffuse reflectance for the noninvasive determination of tissue optical properties *in vivo*," *Med. Phys.* **19**, 879–888 (1992).
3. A. H. Hielscher, J. R. Mourant, and I. J. Bigio, "Influence of particle size and concentration on the diffuse backscattering polarized light from tissue phantoms and biological cell suspensions," *Appl. Opt.* **36**, 125–135 (1997).
4. S. Bartel and A. A. Hielscher, "Monte Carlo simulations of the diffuse backscattering Mueller matrix for highly scattering media," *Appl. Opt.* **39**(10), 1580–1588 (2000).
5. A. Dogariu, M. Dogariu, K. Richardson, S. D. Jacobs, and G. D. Boreman, "Polarization asymmetry in waves backscattering from highly absorbant random media," *Appl. Opt.* **36**(31), 8159–8164 (1997).
6. A. S. Martinez and R. Maynard, "Faraday effect and multiple scattering of light," *Phys. Rev. B* **50**(6), 3714–3732 (1994).
7. G. F. Bohren and D. R. Huffman, *Absorption and Scattering of Light by Small Particles*, Wiley Science PaperBack Series, New York (1998).
8. F. Jaillon and H. Saint-Jalmes, "Description and time reduction of a Monte Carlo to simulate propagation of polarized light through scattering media," *Appl. Opt.* **42**(16), 3290–3296 (2003).
9. L. V. Wang, S. L. Jacques, and L. Zheng, "Monte Carlo modeling of light transport in multi-layered tissues," *Comput. Methods Programs Biomed.* **47**, 131–146 (1995).
10. H. C. van de Hulst, *Light Scattering by Small Particles*, Dover, New York (1981).
11. L. Gobin, L. Blanchot, and H. Saint-Jalmes, "Integrating the digitized backscattered image to measure absorption and reduced scattering coefficients *in vivo*," *Appl. Opt.* **38**(19), 4217–4227 (1999).
12. M. J. Raković and G. W. Kattawar, "Theoretical analysis of polarization patterns from incoherent backscattering of light," *Appl. Opt.* **37**(15), 3333–3338 (1998).